

# Traffic Grooming in Statistically Shared Optical Networks

Srivatsan Balasubramanian and Arun K. Somani  
 Department of Electrical and Computer Engineering  
 Iowa State University, Ames, IA 50011  
 E-mail: {vatsan, arun}@iastate.edu

**Abstract**— We investigate the characteristics and performance of architectures that allow statistical sharing of wavelengths in the optical layer. The bandwidth of a light-wave circuit can be shared in the optical layer by multiple nodes that are along a linear path in a network through the inclusion of simple but flexible hardware overlaid with control software. We consider three types of architectures - lightpath (LP), light-trail (LT) and source based light-trail (SLT) networks. The three differ in their level of optical sharing, in their hardware and software requirements and in their performance. We study the interplay between statistical sharing at the optical layer and circuit switched sharing at the electronic layer. We develop a generic auxiliary graph model for traffic grooming in heterogeneous WDM mesh networks that can accommodate constraints related to transceivers, wavelengths, and groomers for architectures with different levels of statistical sharing and for both static and dynamic scenarios. We conclude based on our simulation results that sharing wavelength in the optical domain is beneficial and can lead to reduced blocking.<sup>1</sup>

## I. INTRODUCTION

Wavelength division multiplexing (WDM) is a promising technology in exploiting the tremendous bandwidth potential latent in fiber. Many switching paradigms have been widely researched as possible architectural choice for the future internet. One such paradigm is the Optical Circuit Switched network (OCS) that creates a dedicated lightpath from source to destination. OCS performs poorly in the presence of sub-wavelength traffic. Traffic grooming improves resource sharing by leveraging fine granular electronic switching capabilities. However, optoelectronic components are expensive at high speeds and can result in networks that are not future proof due to lack of transparency. Optical packet switching can achieve high statistical multiplexing gains but the key components of this network include the switching fabric and optical buffers. The requirement for switches with nanosecond switching times, and the lack of large random access memory units prevent implementation of sophisticated optical router architectures. Optical burst switching is a hybrid approach between coarse-grained circuit switching and fine-grained packet switching. However, this architecture needs either large number of delay lines or wavelength converters. Besides, in burst switching, the ratio of cross-connect configuration time to burst duration may be very high with present optical switching technologies and hence may lead to low network utilization.

An architecture that has sparked interest among the research community was proposed recently in [1] and [2]. The goal of shared wavelength optical networks (SWON) [3] is to eliminate switching on a per packet basis, and leverage resource multiplexing by incorporating a few economically viable hardware components overlaid with a new control protocol to achieve high network utilization (to be described later). Such architectures present a paradigm that is positioned between OCS and OBS technologies. The static routing and wavelength assignment (RWA) problem in such networks was formulated as ILP and heuristics were studied in [4]. Simple medium access control protocols (MAC) for wavelength sharing were introduced in [1], [5], [6], [7]. Survivable design of shared optical networks were researched in [8], [9]. A streaming media application was demonstrated on a 3 Gbps optical testbed deploying SWON architecture in [10].

The combined effect of circuit switched electronic sharing (electronic grooming) and statistically multiplexed optical sharing was studied first in [11]. The work in [11] introduces an auxiliary graph approach to solve the traffic grooming problem in a specific type of SWON called light-trails (to be explained later). This model scales with number of network links while the model we present here scales with the number of network nodes. Our model can be applied to multiple types of SWONs unlike the earlier work which works for light-trails. Besides, [11] focused only on the service provisioning aspects. The objective of this paper is to introduce six different metrics and compare the performance of various grooming and non-grooming SWON architectures for these various metrics.

The rest of the paper is organized as follows. Section II introduces the SWON architecture and identifies the three types of SWONs we investigate in this work. Section III discusses a generic grooming switch design for SWON architectures. A five node sample network scenario in which a sequence of calls need to be routed are provided in Section IV, and the resource requirements of various architectures for carrying this traffic are analyzed. The auxiliary graph based model is introduced in section V and a small three node network example has been worked out to illustrate the grooming heuristic. In section VI, the simulation results are described. Finally, in section VII, we conclude our paper with possible future work.

## II. SWON DATA PLANE

Figure 1(a) shows a lightwave circuit [1] established between first node (convener node) and the fourth node (end node) on

<sup>1</sup>The reported research is funded in part by NSF under grant ANI-0087746, ANI-0434872 and ANI-0306007

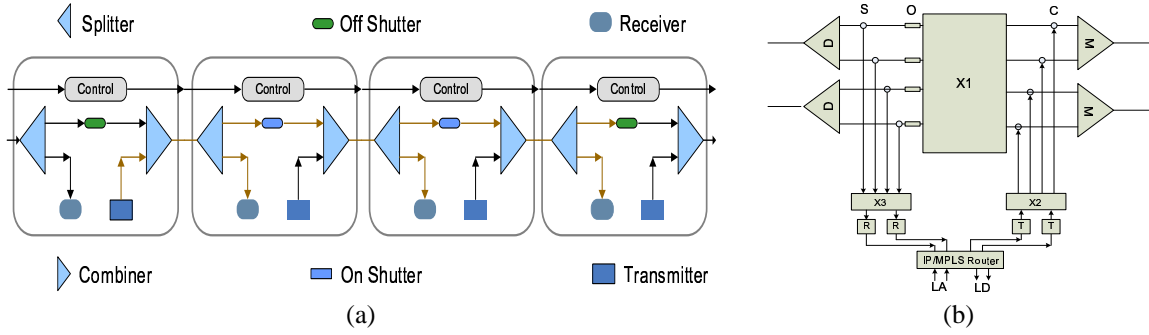


Fig. 1. (a) Node architecture for a single wavelength SWON. (b) Partial grooming architecture for light-trail networks. D - Demultiplexer, M - Multiplexer, O - Optical Shutter, X1,X2,X3 - OXC, T - Transmitter, R - Receiver, LA - Local Add, LD - Local Drop, S - Splitter, C - Combiner

a single wavelength ring (not fully shown). This circuit allows wavelength sharing at the optical layer among multiple nodes that reside on circuit's path using a simple carrier-sensing MAC protocol discussed in [1], [5], [6], [7]. Each node consists of a splitter, a shutter and a combiner. A packet sourced from a node on this circuit traverses each of these optical components on every node en route to the end node. At the splitter of a node, a part of the incoming signal power is sent to the local node for possible reception using a detector while the rest of the signal passes to the shutter. The shutter is a simple mirror-based optical attenuator configured to either block or let the wavelength pass through. For the first and last node on the circuit, the shutter is configured in the off/blocking position, isolating this wavelength from the rest of the network. For intermediate nodes on the circuit, the shutter is in the on/pass-through position, letting the signal pass through. The signal, if not blocked by the shutter, travels through the combiner before exiting the node. The combiner allows the data sourced by the intermediate node to be coupled into the wavelength based on some MAC strategy.

The architecture utilizes an out of band control channel, which is dropped and processed at each node to actuate the shutters. The signaling channel carries information pertaining to circuit set up, tear down and dimensioning, and can provision optical connections, ranging in duration from IP bursts to virtual circuits [1]. The shutters are not reconfigured dynamically for every packet but is done on a longer time scale thereby alleviating the switching speed requirement. This statistical sharing of a circuit leads to a better utilization of wavelength in the presence of heavily fractional traffic.

Consider a network topology as a directed graph  $G(V, E)$ , with  $V$  as the vertex set and  $E$  as the edge set. Let  $C$  be a simple path in a graph defined by the sequence  $C = \{v_1, v_2, \dots, v_n\}$  such that  $v_1, v_2, \dots, v_n \in V$  and  $(v_1, v_2), (v_2, v_3), \dots, (v_{n-1}, v_n) \in E$ .  $v_1$  is the convener node and  $v_n$  is the end node. Connections can be carried by the lightwave circuit  $C$  based on the capacity constraint and the containment constraint. The capacity constraint is that the sum of the requests supported by a shared wavelength circuit is no more than the capacity of a wavelength. The containment constraints refer to the type of connections that can be multiplexed onto a wavelength. Based on this, we define the following three types of SWONs.

- Light-trail ( $LT$ ): If the containment set is  $\{(v_i, v_j) : v_j$  is

downstream of  $v_i$  on  $C\}$ , we refer to the resulting SWON type as the light-trail architecture and has been the subject of research in [1]-[11].

- Source based light-trail ( $SLT$ ): If the containment set is  $\{(v_1, v_j) : v_j$  is downstream of  $v_1$  on  $C\}$ , we refer to the resulting SWON type as the source based light-trail architecture and a variant of it has been studied in [12].
- Lightpath ( $LP$ ): If the containment set is  $\{(v_1, v_n)\}$ , it can share only the connections between the convener node and the end node and the resulting architecture is similar to the single hop lightpath architecture described in [14].

It can be seen that  $LP$  is a special case of  $SLT$  which in turn is a special case of  $LT$ . Each architecture differs in its hardware and software requirements.  $LT$ s require all the hardware shown in Figure 1 and a MAC protocol.  $SLT$ s can be implemented with lesser hardware [12] since only one node can source data on an  $SLT$  circuit. Besides, for  $SLT$ , the connections headed for multiple destinations are scheduled locally on the convener node based on some queuing policy and consequently there is no requirement for a distributed MAC protocol. The  $LP$  architecture does not require the above mentioned hardware and MAC protocol. For a more detailed discussion on SWON architectures, readers are referred to [13] which is the complete version of this paper.

### III. SWON CONTROL PLANE

Based on the above mentioned model, resources can be shared by nodes along a simple path. Architectures, where resources can be shared on a tree as in [14] are beyond the scope of this work. It may be useful to overlay a circuit switched electronic sharing scheme (by introducing a grooming fabric) and investigate its interplay with the statistical grooming scheme already present in the optical layer for the three SWON architectures. Towards this objective, we design a heuristic that solves the routing and wavelength assignment (RWA) problem and the connection routing problem in an integrated fashion for the three types of SWONs.

For details on call set up and call tear down procedures in SWON architectures, readers are referred to [1]. We describe here the concept of 'tune-in' light trails introduced in [11]. When a new circuit needs to be established, only the transmitter on the source and the receiver on the destination are provisioned. During trail operation, if a node wants to source

(sink) data, it will first check if it already has a transmitter (receiver) tuned into the trail. If this unit exists, it will be used for transmitting (receiving) data. Otherwise, a freely available transmitter (receiver) on the node is 'tuned in' to the trail. This ensures that only minimal equipment are utilized.

Figure 1(b) shows a grooming switch architecture which allows for up to 4 wavelengths to be shared. It allows the transmitters and receivers to be used independently. Consider a node that is active on four trails ( $T_1, T_2, T_3$  and  $T_4$ ), where it transmits only on  $T_1$  and  $T_2$  and receives only on  $T_3$  and  $T_4$ . Assume that traffic from  $T_4$  needs to be groomed onto  $T_1$ . The four trails are tapped at the local node, but  $T_3$  and  $T_4$  are selected by X3 to be detected at the two receivers. All the four trails continue through the splitter(S), shutter(O) and the combiner(C). Signals from the two local transmitters are switched by X2 to trails  $T_1$  and  $T_2$ . Please note that a MAC unit is required to access the channel (not shown in the figure). The IP/MPLS router grooms connections across trails through a software based queueing scheme. This grooming architecture can be extended to model *SLT* based networks as well and we do not present it here for lack of space. A survey of grooming architectures in LP networks is provided in [14].

#### IV. RESOURCE CONSUMPTION IN SWONS

In this section, we consider an example five node network and identify the resource requirements of various architectures for a specified sequence of five call arrivals. We study the above mentioned three architectures along with their groomable counterparts. Let  $C_{s,d}^i$  refer to the  $i^{th}$  connection in the sequence of dynamic arrivals, and the connection is to be established between  $s$  and  $d$ . Assume each arrival has size 3 units, the wavelength to be of capacity 12 units and that arrived calls do not depart. We explain only Figure 3(b) for SLT-TG network that refers to an SLT network with all nodes having full traffic grooming (TG) capabilities. When  $C_{0,2}^1$  arrives at the network, a circuit  $X_{012}$  is established and the corresponding communication equipment are provisioned. The next call to arrive is  $C_{0,1}^2$ . This is accommodated by having a node 1 receiver 'tune into' the  $X_{012}$  circuit. Suppose that connection  $C_{1,3}^3$  arrives at the network now. This can be routed on the network through a new circuit  $X_{123}$ . When the next connection  $C_{1,2}^4$  arrives, the receiver of node 2 is tuned into  $X_{123}$ . The final connection to arrive is  $C_{0,3}^5$ . Since, grooming is available on every node, this connection can be routed from node 0 over  $X_{012}$  to be terminated at node 1 and then switched over to  $X_{123}$  to be finally received at node 3.

This example brings up two important observations. Firstly, node 1 is able to groom the data obtained from node 0 and send it towards node 3. This is possible only because intermediate nodes on an SLT circuit can receive data and this feature is absent in LP circuits. It leads us to believe that LT-TG and SLT-TG networks may have superior grooming capabilities than LP-TG networks. Secondly, any data that node 0 sends towards node 1 ends up locking an equivalent amount of bandwidth on the link (1, 2) (since this link is a part of the circuit), though node 2 may not be interested in this data. We call this 'bandwidth locking' and it is an inherent inefficiency in the

proposed sharing mechanism which is absent in LP networks. In the present example, to accommodate all the five calls, the network requires a total of two wavelengths, two transmitters and four receivers. The call arrival sequence is the same for all the other architectures and their resource requirements are summarized in Figure 3 (d).

#### V. TRAFFIC GROOMING ALGORITHM FOR SWONS

It is clear from the above example that different architectures lead to different levels of performance. We investigate this for larger networks by designing a generic graph model for dynamic traffic grooming in mesh networks with six different architectures. The basic idea behind our approach is as follows. We design an algorithm that takes traffic request  $T(s, d, m)$  as input, where  $m$  is the value of the subwavelength request between source  $s$  and destination  $d$ . An auxiliary graph is obtained based on the current network state taking into account the availability of grooming switches, transceivers, wavelengths and their respective costs. The cost of resources are assigned based on a chosen grooming policy. Using Dijkstra's algorithm, the shortest route is identified between  $s$  and  $d$  that can accommodate the request  $m$ . If the required resources in terms of wavelengths, transceivers and switching ports are not available in the network, the call is blocked. Otherwise, the network state is modified to reflect the resources consumed by admitting the current request and the algorithm proceeds to handle the next traffic request. In a dynamic scenario, the objective of any RWA algorithm is typically to maximize the acceptance likelihood for an incoming call and simultaneously attempt to minimize blocking probability for future requests.

In this section, we introduce the auxiliary graph and outline the various steps of the algorithm. We describe the algorithm for LT-TG (referred to as trails below), though it will be shown that with minor modifications other architectures can be modeled. Next, we illustrate the heuristic with some examples. Subsequently, we identify the grooming policy and assign costs to network resources to achieve the required objectives. It is assumed that every node in the network maintains complete topology and wavelength state information through link state updates.

##### A. Auxiliary graph generation

The physical topology of a network can be represented by a graph  $G'(V', E')$  where  $V'$  is the node set and  $E'$  is the link set. The corresponding auxiliary graph is defined as  $G(V, E)$  with  $(2W + 6)V'$  vertices and is generated as follows. In  $G$ , each node comprises of  $W + 3$  layers with each layer including an input port and an output port. Layers 1 through  $W$  are the Wavelength layers (*WLs*), layer  $W + 1$  and layer  $W + 2$  are the Trail layers (*TLs*), and layer  $W + 3$  is the Grooming layer (*GL*). Let  $V_y^{i,k}$  refer to the  $y^{th}$  port on layer  $k$  at node  $i$ . Let  $y = 1$  refer to the input port and  $y = 0$  refer to the output port. The edges are inserted in the auxiliary graph as follows:

- Grooming edge: For each node  $i$  that is grooming capable, an edge is introduced from the input port to the output port of the Grooming Layer. That is,

$$(V_1^{i,W+3}, V_0^{i,W+3}) \in E \quad \forall i \in V' \quad (1)$$

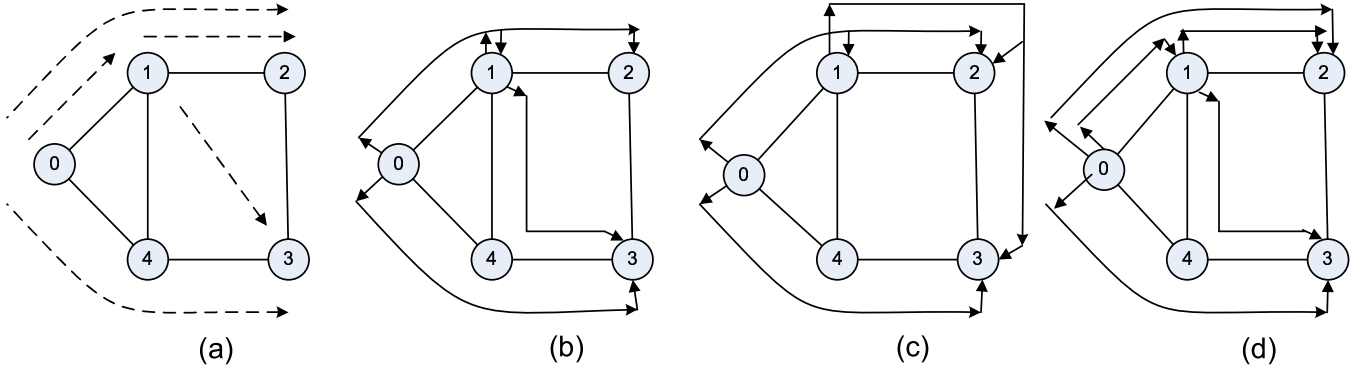


Fig. 2. (a) Dynamic requests (b) **LT**:  $X_{13} = \{C_{1,3}^3\}$ ,  $X_{012} = \{C_{0,1}^2, C_{1,2}^4, C_{0,2}^1\}$ ,  $X_{043} = \{C_{1,3}^3\}$  (c) **SLT**:  $X_{012} = \{C_{0,1}^2, C_{0,2}^1\}$ ,  $X_{123} = \{C_{1,2}^4, C_{1,3}^3\}$ ,  $X_{043} = \{C_{0,3}^5\}$  (d) **LP**:  $X_{01} = \{C_{0,1}^2\}$ ,  $X_{12} = \{C_{1,2}^4\}$ ,  $X_{012} = \{C_{0,2}^1\}$ ,  $X_{143} = \{C_{1,3}^3\}$ ,  $X_{043} = \{C_{0,3}^5\}$

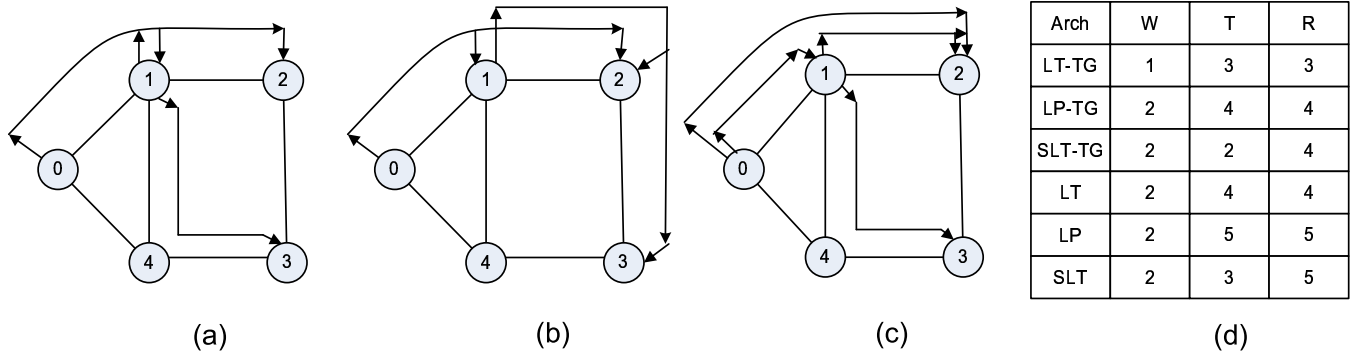


Fig. 3. (a) **LT-TG**:  $X_{012} = \{C_{0,1}^2, C_{1,3}^3, C_{0,2}^1, C_{0,3}^5\}$ ,  $X_{143} = \{C_{1,2}^4, C_{0,3}^5\}$  (b) **SLT-TG**:  $X_{012} = \{C_{0,1}^2, C_{0,2}^1, C_{0,3}^5\}$ ,  $X_{123} = \{C_{1,3}^3, C_{0,3}^5, C_{1,2}^4\}$  (c) **LP-TG**:  $X_{012} = \{C_{0,2}^1\}$ ,  $X_{01} = \{C_{0,1}^2, C_{0,3}^5\}$ ,  $X_{12} = \{C_{1,2}^4\}$ ,  $X_{143} = \{C_{1,3}^3, C_{0,3}^5\}$  (d) Summary of resource requirements

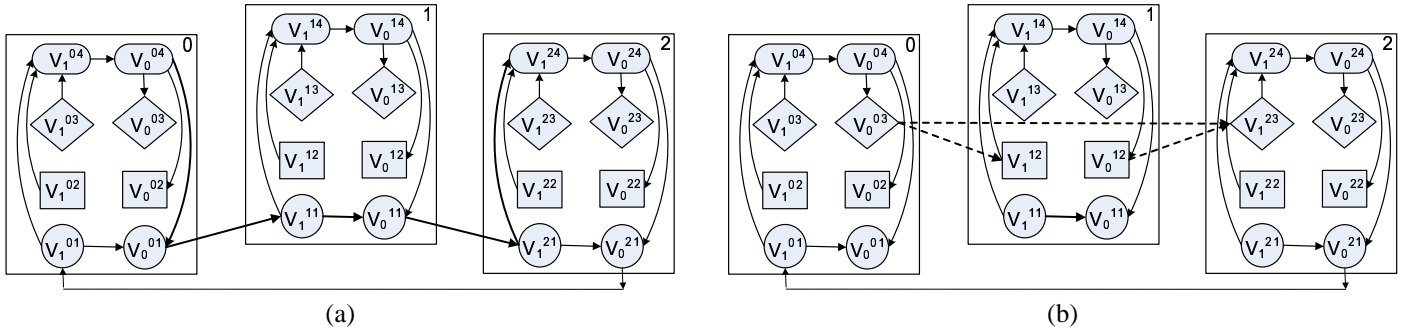


Fig. 4. (a) Three node single wavelength unidirectional LT-TG ring (b) Connection from node 0 to node 2 is set up on trail  $\{0,1,2\}$

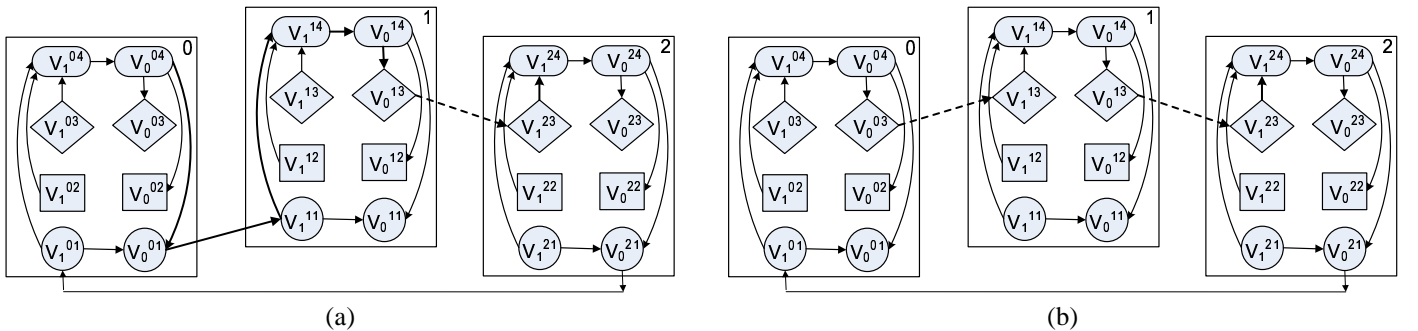


Fig. 5. (a) Connection from node 0 to node 2 is torn down. Connection from node 1 to node 2 remains. (b) New connection from node 0 to node 2 is admitted. New trail  $\{0,1\}$  is set up and connection groomed through node 1

- Wavelength link edge: If a free wavelength  $k$  exists on the link  $(i, j)$ , an edge is introduced between the output port of wavelength layer  $k$  on node  $i$  and the input port of wavelength layer  $k$  on node  $j$ . That is,

$$(V_0^{i,k}, V_1^{j,k}) \in E \quad \forall (i, j) \in G',$$

$$\text{wavelength } k \text{ is free on } (i, j) \quad (2)$$

- Trail edge: Let  $z$  denote a communication unit on a node with  $z = 0$  referring to a transmitter and  $z = 1$  referring to a receiver. Let  $T_t$  refer to the  $t^{\text{th}}$  trail in the network. If  $i \in T_t$ , node  $i$  is active on the trail. Define  $A_t^z(i) = 1$  if  $i \in T_t$  and node  $i$ 's  $z^{\text{th}}$  communication unit is active on  $T_t$ ; 0 if  $i \in T_t$  and node  $i$ 's  $z^{\text{th}}$  communication unit is idle on  $T_t$ ; -1 otherwise. Let  $I_t(j)$  refer to the location of node  $j$  in trail  $T_t$ . Four kinds of edges are introduced for *LT* networks based on the following conditions.

$$(V_0^{i,W+1}, V_1^{j,W+1}) \in E, \text{ for some trail } t \text{ carried in } G,$$

$$\forall i, j : A_t^0(i) = 0, A_t^1(j) = 0, I_t(j) > I_t(i) \quad (3)$$

$$(V_0^{i,W+1}, V_1^{j,W+2}) \in E, \text{ for some trail } t \text{ carried in } G,$$

$$\forall i, j : A_t^0(i) = 0, A_t^1(j) = 1, I_t(j) > I_t(i) \quad (4)$$

$$(V_0^{i,W+2}, V_1^{j,W+1}) \in E, \text{ for some trail } t \text{ carried in } G,$$

$$\forall i, j : A_t^0(i) = 1, A_t^1(j) = 0, I_t(j) > I_t(i) \quad (5)$$

$$(V_0^{i,W+2}, V_1^{j,W+2}) \in E, \text{ for some trail } t \text{ carried in } G,$$

$$\forall i, j : A_t^0(i) = 1, A_t^1(j) = 1, I_t(j) > I_t(i) \quad (6)$$

Equation (6) states that if  $i$ 's transmitter unit is active on  $t$ ,  $j$ 's receiver unit is active on  $t$  and  $j$  is downstream of  $i$  on trail  $t$ , an edge is introduced from output port of layer  $W + 2$  on node  $i$  to input port of layer  $W + 2$  on node  $j$ . Similar interpretations can be extended for the other equations as well. A more detailed description of trail edges will be illustrated using an example in a later section. The above mentioned equations are true only for *LT* and *LT-TG* networks. For modeling *SLT* and *SLT-TG* networks, include the additional constraint that  $i$  should be the convener node for trail  $t$  for Eqs (3) to Eqs (6). For modeling *LP* and *LP-TG* networks, include the constraint that  $i$  should be the convener node and  $j$  should be the end node for trail  $t$  for Eqs (3) to Eqs (6).

- Mux edge: There is an edge introduced between the output port of layer  $W + 3$  on node  $i$  to output port of layer  $W + 2$  on node  $i$ .

$$(V_0^{i,W+3}, V_0^{i,W+2}) \in E \quad \forall i \in V' \quad (7)$$

- Demux edge: There is an edge introduced between the input port of layer  $W + 2$  on node  $i$  to input port of layer  $W + 3$  on node  $i$ .

$$(V_1^{i,W+2}, V_1^{i,W+3}) \in E \quad \forall i \in V' \quad (8)$$

- Receiver edge: If there is at least one free receiver available at node  $i$ , two types of arcs are introduced. First, there is an edge introduced from the input port of every *WL* at node  $i$  to the input port of *GL* at node  $i$ . Second,

an edge is introduced between input port of layer  $W + 1$  at node  $i$  to input port of *GL* at node  $i$ .

$$(V_1^{i,k}, V_1^{i,W+3}) \in E \quad \forall i \in V', k \in \{1, ..W\} \quad (9)$$

$$(V_1^{i,W+1}, V_1^{i,W+3}) \in E \quad \forall i \in V' \quad (10)$$

- Transmitter edge: If there is at least one free transmitter available at node  $i$ , two types of arcs are introduced. First, there is an edge introduced between output port of *GL* at node  $i$  to output port of every *WL* at node  $i$ . Second, there is an edge introduced between output port of *GL* at node  $i$  to output port of layer  $W + 1$  at node  $i$ .

$$(V_0^{i,W+3}, V_0^{i,k}) \in E \quad \forall i \in V', k \in 1, ..W \quad (11)$$

$$(V_0^{i,W+3}, V_0^{i,W+1}) \in E \quad \forall i \in V' \quad (12)$$

- Wavelength bypass edge: There is an edge from the input to the output port of each wavelength layer at node  $i$ .

$$(V_1^{i,k}, V_0^{i,k}) \in E \quad \forall i \in V', k \in \{1..W\}$$

Each edge  $(i, j)$  in the auxiliary graph is associated with a tuple  $\{c_{i,j}, w_{i,j}\}$ , where  $c_{i,j}$  is its residual capacity and  $w_{i,j}$  is its cost. The  $c_{i,j}$  of a wavelength edge is the capacity of a wavelength. For the trail edge, it is the residual capacity of the trail. For all the other edges,  $c_{i,j}$  is assigned to be infinity. The trail edges also carry the required *RWA* information.  $c_{i,j}$  can reflect the actual cost of a network element and/or the requirements of a grooming policy.

The algorithm is described in detail in [13]. The input to the algorithm is the current network state in the form of the auxiliary graph generated. The method takes a request  $T(s, d, m, t_a, t_e)$ , where  $t_a$  is the arrival time and  $t_e$  is the exit time of the call, runs a shortest route algorithm on the auxiliary graph from the output port of *GL* on node  $s$  to the input port of *GL* on node  $d$ . If the path exists, the call is accepted, *RWA* is performed, and the auxiliary graph is updated. Otherwise, the call is blocked. The running time of this algorithm is  $O(E \log V)$ .

This model can achieve various objectives using different grooming policies. A chosen request can be routed on a network in many ways. The route generated by Dijkstra's algorithm could be one of the following: (a) It is a direct trail from source to destination. (b) It is a concatenation of multiple trails from source to destination. (c) It is a concatenation of multiple free wavelength links from source to destination. (d) It is a concatenation of both trails and free wavelength links from source to destination.

It is possible that we may prefer one of the routes over the other for carrying traffic and this reflects the chosen grooming policy. Typically, we specify a grooming policy for network operation in terms of the parameter we want to optimize and try to achieve it by prioritizing the route selection process and greedily applying it to every request carried by the network as explained in [15]. We could identify multiple grooming policies with objectives like minimizing the number of virtual hops, minimizing network costs or minimizing service provisioning time. Each of these can be achieved based on assigning priorities to the type of path that we want to choose. Due

to lack of space, we consider only one grooming policy which aims to minimize the total number of physical hops. We do this by obtaining paths of all four types and choosing the one with minimum number of physical hops. Since we would like to encourage grooming, we assign unit cost to a Mux(Demux) edge that represents a transmitter(receiver) already in use and a cost of 10 to transmitter and receiver arcs. We assign a unit cost to wavelength link edge and grooming edge while we assign the cost of the trail edge to be the physical hop length of the trail.

### B. Illustrative example

We describe the auxiliary graph generation procedure using a single wavelength, three node unidirectional LT-TG ring  $\{0,1,2,0\}$ . All connections that arrive have half the capacity of the wavelength and hence two of them can share one wavelength. Initially, no trail is set up in the network. Assume that a connection  $C_{0,2}^1$  arrives. This request can be routed through the available free wavelength links on the route  $T_1 = \{0,1,2\}$  shown in Figure 4(a). As a result, free wavelength links  $(V_0^{0,1}, V_1^{1,1})$  and  $(V_0^{1,1}, V_1^{2,1})$  are removed and a trail edge  $(V_0^{0,3}, V_1^{2,3})$  is introduced in  $G$ .

The newly established trail can accommodate the request (0,1) or (0,2) or (1,2) in the future. The trail edge that was just introduced offers connectivity in the auxiliary graph to support only the request (0,1) in the future. To include the additional reachability information, two additional edges  $(V_0^{0,3}, V_1^{1,2})$  and  $(V_0^{1,2}, V_1^{2,3})$  are introduced as seen in Figure 4(b). The communication unit of a node on a trail could be either in the idle (not provisioned) state or in the active (provisioned) state. In some sense, layer 3 refers to the active state while layer 2 refers to the idle state. The layer at which a trail edge originates and terminates on a node depends on the state of the corresponding node's transmission and reception units respectively. For instance, node 1's transmitter and receiver units are idle on the trail while node 0's transmitter and node 2's receiver are active on the trail as shown in Figure 4(b). The three trail edges are identified with the same trail and the capacity of the edges is assigned the residual capacity of the trail. The properties (like capacity) of all the three edges are updated as requests are set up or torn down on the trail.

Assume that another connection  $C_{1,2}^2$  arrives. This request can be routed on the residual capacity of the existing trail  $T_1$  and requires a new transmitter on node 1 to be activated. Since the state of the transmission unit of node 1 on trail  $T_1$  has changed, the trail edge  $(V_0^{1,2}, V_1^{2,3})$  is removed and a new edge  $(V_0^{1,3}, V_1^{2,3})$  is introduced. The residual capacity on all trail edges are updated. Let us consider two cases.

In the first case,  $C_{1,2}^2$  leaves before  $C_{0,2}^1$ , making node 1 transmitter idle on  $T_1$ . The edge  $(V_0^{1,3}, V_1^{2,3})$  is removed, the edge  $(V_0^{1,2}, V_1^{2,3})$  is added, making it consistent with eq (5) and the capacity of all edges are updated. If  $C_{0,2}^1$  leaves before another connection arrives, all the trail edges are removed and the original wavelength links are replaced.

In the second case,  $C_{0,2}^1$  leaves before  $C_{1,2}^2$ , the wavelength link (0,1) in the trail  $T_1$  is free. Control plane signaling could be used to dimension the trail and  $T_1$  is modified to  $\{1,2\}$ . The

trail edges  $(V_0^{0,3}, V_1^{2,3})$  and  $(V_0^{0,3}, V_1^{1,2})$  are removed and the wavelength edge  $(V_0^{0,1}, V_1^{1,1})$  is added as observed in Figure 5(a). Now, a new connection  $C_{0,2}^3$  arrives. The connection can be carried from node 0 to node 1 using the just freed wavelength link (0,1) creating a new trail  $T_2 = \{0,1\}$ , and then be electronically groomed by node 1 to be multiplexed along with trail  $T_1$  to reach node 2. This activates the transmitter on node 0 and the receiver on node 1. Hence new trail edges  $(V_0^{0,3}, V_1^{1,3})$  is added and the wavelength edge  $(V_0^{0,1}, V_1^{1,1})$  is removed as seen in Figure 5(b).

## VI. SIMULATION RESULTS

### A. Performance Metrics

Below, we define performance metrics of interest [13]:

- Wavelength Usage ( $U_w$ ): This is the weighted ratio of the average number of used wavelength links to the total number of wavelength links provisioned in the network.
- Wavelength packing fraction ( $F_w$ ): This is the average fraction of the capacity of a wavelength in use that carries useful traffic throughout the period of simulation.
- Transceiver Usage ( $U_x$ ): This is the ratio of the number of transceivers used to the number of transceivers provisioned in the network over the simulation period.
- Transceiver packing fraction ( $F_x$ ): This is the average fraction of the capacity of transceiver in use that carries useful traffic throughout the simulation period.
- Bandwidth blocking probability ( $B$ ): This refers to the fraction of the calls blocked weighted by the capacity requirement of the call.
- Network load ( $L$ ): This is the ratio of the average arrival rate ( $\lambda$ ) to the average departure rate ( $\mu$ ).

### B. Results and Discussion

We compare the performance of six different architectures on a random mesh topology which has 20 nodes, 39 bidirectional links, diameter of 5 and an average path length of 2.5. Each wavelength has a capacity of 48 units and wavelength conversion is absent. The call arrival is a Poisson distributed and call holding time is exponentially distributed (with average value normalized to unity). The traffic is uniformly distributed among all node pairs. There are three types of connection requests classified based on their sizes - 3, 12 and 48 units. Their probability distribution is such that, if combined capacity of calls to a node pair is  $Kg$ , where  $g$  is the number of distinct granularities, each line speed contributes a capacity of  $K$  through its arrivals. We simulate 100,000 requests on a 3 GHz Pentium IV processor and 512 MB RAM to obtain the network performance results which takes upto a maximum of 5 minutes to run. All the results reported in this section except for Figure 6 (a) are obtained with values  $W=5$  and  $X=5$ .

The results shown in Figure 6(a) corresponds to all-optical LT networks. The blocking probability ( $B$ ) is plotted as a function of  $X$  and  $W$  for a load of 50 Erlangs. It is observed that  $B$  is more sensitive to changes in  $X$  than in  $W$ . When  $X = 5$ , increase in value of  $W$  even upto 8 does not change  $B$  greatly since it becomes a transceiver constrained system. Similarly,

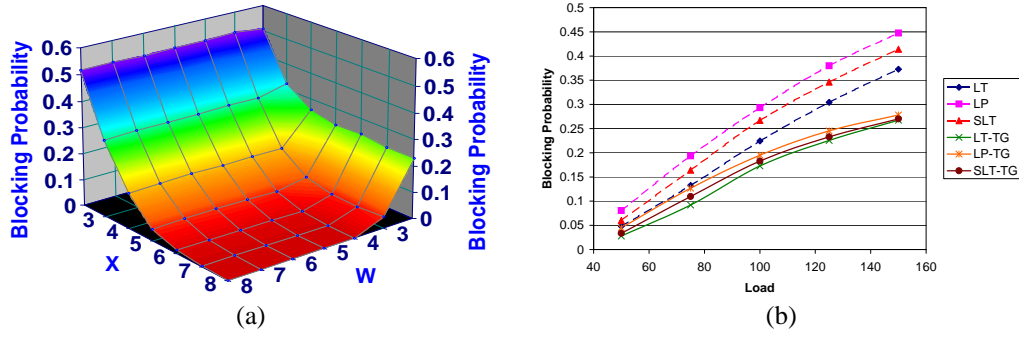


Fig. 6. (a) Blocking Probability as a function of X and W for LT architecture when load = 50 Erlangs (b) Blocking Probability Vs Load at (X=5,W=5) for all architectures

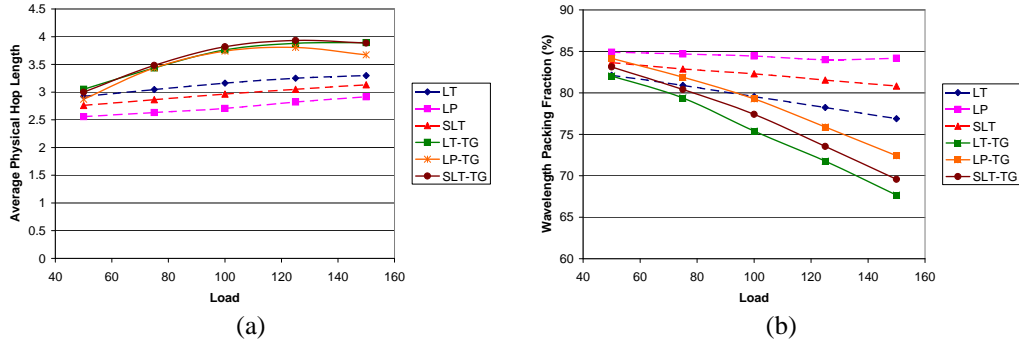


Fig. 7. (a) Average physical hop length per connection Vs Load at (X=5,W=5) (b) Wavelength packing fraction Vs Load for all architectures at (X=5,W=5)

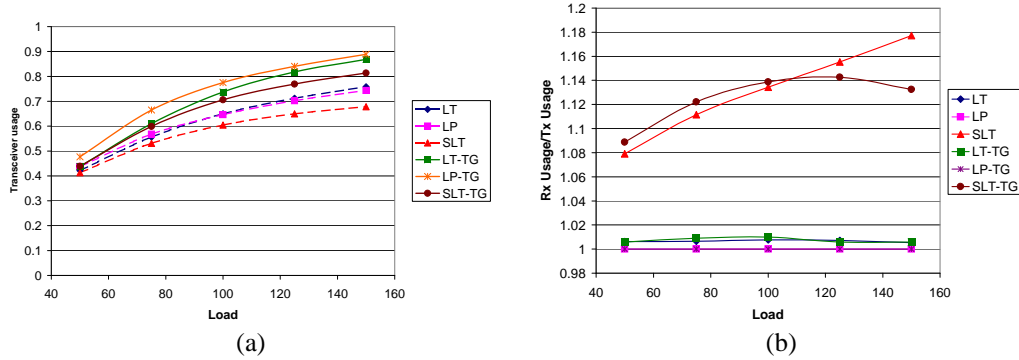


Fig. 8. (a) Transmitter usage Vs Load for all architectures at (X=5,W=5) (b) The ratio of receiver usage to transmitter usage as a function of load at (X=5,W=5)

when  $W = 2$ , irrespective of the increase in  $X$ ,  $B$  does not change since it is a wavelength constrained system. Blocking is higher for higher granularity (graph shown in [13]) since the likelihood of residual capacity in the network being higher is smaller. Blocking is same for 3 units request and 12 units request while it is much higher for 48 units request [13].

$B$  is plotted as a function of load for all the six different architectures in Figure 6(b). Blocking increases with increase in load and grooming architectures outperform non grooming architectures. Since  $LT$  offers most number of options for sharing,  $B_{LT} < B_{SLT} < B_{LP}$ . Typically, bandwidth blocking beyond 1% is unacceptable in commercial networks, but we show a wide range of  $B$  values for the sake of completeness. The difference between grooming and non grooming counterparts is not significant in this scenario since one of the granularity we have chosen is 48 units which cannot be

groomed. With lesser number of connections to be groomed, the impact of grooming reduces.

The average value of physical hop length is plotted as a function of load in Figure 7(a). There is a tight coupling between physical hop length and blocking for grooming networks. When grooming is efficient, more number of connections are admitted and blocking decreases. However, the admitted connections take longer routes due to unavailability of shorter routes. This leads to wastage of bandwidth and there is a consequent increase in blocking. In general, grooming networks have more options while routing and accept longer connections than non-grooming networks. For non-grooming networks, as load increases, more number of calls are dropped and probabilistically calls with longer path lengths are more likely to be blocked. Hence, the average physical length per accepted connection would be expected to decrease. However,

with increase in load, the connections take longer routes due to unavailability of shorter routes. Hence, the average physical length per connection would increase as well. The result of these two conflicting factors is that we observe that there is a small increase in PL as load increases. It is observed that at low loads, LP architectures have PL values close to the topology's average path length. The bandwidth locking problem in LT and SLT networks increases the physical length of a connection since the PL of a connection is the length of the circuit (which is typically longer) that supports the connection.

The wavelength packing fraction as a function of load is seen in Figure 7(b). In general, most of the wavelengths are packed up to about 95 % for small loads and packing fraction drops quickly as load increases. Also, packing fraction seen in non-grooming networks is better than in the corresponding grooming counterparts. To understand this, the variation of wavelength usage as a function of load (graph not shown for lack of space) needs to be analyzed. It was observed that grooming networks used more more wavelengths than non-grooming networks and wavelength usage increased with increase in load for all architectures. More wavelengths were used by grooming networks because they carried more traffic. With high loads, new wavelengths are rapidly opened up for all architectures due to increased inflow of connections. Consequently, the wavelength usage increases from approximately 30 % at 50 Erlangs to about 50 % at 150 Erlangs. When wavelength usage increases, there is lesser likelihood of efficient packing and hence packing fraction drops.

Figure 8(a) plots the ratio of receiver usage to transmitter usage as a function of load. In SLT and SLT-TG circuits, there is one transmitter and multiple receivers leading to better packing on transmitters. We see about 15 % more usage of receivers as compared with transmitters at high loads. It is likely that blocking in such networks are a result of receiver exhaustion rather than transmitter exhaustion. This observation gains significance in light of the fact that receivers are cheaper than transmitters. Since our grooming architecture allows independent control of receivers and transmitters, more receivers than transmitters can be provisioned to reduce blocking.

The transmitter usage ( $U_t$ ) is plotted in Figure 8(b). For a given carried traffic, it is better to consume lesser transmitters since this implies a larger network residual capacity. For a given load, grooming architectures carry more traffic and hence has higher  $U_t$ . In general, SLT and SLT-TG architectures have lower  $U_t$  values due to the single source multiple destination paradigm that allows more efficient transmitter packing. However, SLT and SLT-TG lead to highest receiver usage (graphs not shown for lack of space). At high loads, close to 90 % of the transmitters are used in grooming architectures. However, the packing fraction value of each used transmitter or receiver (graph not shown for lack of space) reveals that approximately only about 20 % of each communication unit has been utilized for carrying actual traffic.

A general observation is that transceivers are consumed rapidly but packed sparsely while wavelengths are consumed sparsely but packed densely. This can be explained as follows. A wavelength is a link resource while a transceiver is a node resource. For every participating connection on a circuit, the

specified sharing mechanism improves the packing of link resource. However, the packing of node resource increases only under certain conditions. Consider a four node circuit  $\{A,B,C,D\}$  that carries request A to D. If a connection from B to C arrives and is shared on the existing circuit, the circuit packing improves, but the transceiver packing on any node has not improved. However, if the second connection were from A to C in stead of B to C, the transmitter packing on A would also improve. It is clear that the proposed sharing mechanism always leads to better wavelength packing but leads to better transceiver packing only under certain conditions.

## VII. CONCLUSIONS

The study is focused on traffic grooming in networks deploying statistical sharing at the optical layer. We focused on three types of SWON architectures, and investigated the impact of circuit switched electronic sharing in such systems. We designed and implemented our traffic grooming heuristic on a 20 node mesh network and reported our findings. We observed that LT and SLT networks provide lower blocking than LP networks. Also, LT-TG and SLT-TG outperform LP-TG networks. For SLTs, we see upto 15 % more receivers being used than transmitters thereby suggesting that an assymetric provisioning of transmitters and receivers would improve its performance. The sharing mechanism leads to very efficient wavelength packing and a modest improvement in transceiver packing. We intend to investigate SWONs for topologies with different connectivities in the presence of sparse and partial grooming scenarios, which will help us quantify the benefits of statistical wavelength sharing better.

## REFERENCES

- [1] A. Gumaste, and I. Chlamtac, *Light-trails: an optical solution for IP transport*, Journal of optical networking, Vol. 3, No.4, April 2004.
- [2] N.Le. Sauze et al, *A novel, low cost optical packet metropolitan ring architecture*, in Proc. ECOC, Vol 4, Oct 2001.
- [3] A. Gumaste, et al, *Performance Evaluation and Demonstration of Light-trails in Shared Wavelength Optical Networks (SWON)*, 31st ECOC 2005.
- [4] S. Balasubramanian, A.E. Kamal, A.K. Somani, *Network design in IP-Centric light-trail networks*, IEEE Broadnets 2005.
- [5] S. Balasubramanian et al, *Medium Access Control Protocols For light-trail and Light Bus Networks*, IFIP ONDM 2004.
- [6] N.Bouabdallah, *Resolving the fairness issues in bus-based optical access networks*, IEEE JSAC, Vol 23, No 8, August 2005
- [7] D. Kliazovich et al, *Bidirectional light-trails for synchronous communications in WDM networks*, IEEE Globecom 2005
- [8] S. Balasubramanian, W. He, A.K. Somani, *Light-Trail Networks: Design and Survivability*, IEEE LCN 2005.
- [9] W. Zhang, G. Xue, J. Tang, K. Thulasiraman, *Dynamic light trail routing and protection issues in WDM optical networks*, IEEE Globecom 2005
- [10] N. VanderHorn et al, *Light-Trail Test Bed for IP-Centric Applications*, IEEE Communications Magazine, August 2005
- [11] Y. Ye, H. Woesner, R. Grasso, T. Chen, I. Chlamtac, *Traffic grooming in light trail networks*, IEEE Globecom 2005
- [12] F. Farahmand et al, *Efficient Online Traffic Grooming Algorithms in WDM Mesh Networks with Drop-and-Continue Node Architecture*, in IEEE BroadNets 2004, San Jose, CA, October 2004.
- [13] S. Balasubramanian, A.K. Somani, *Traffic grooming in statistically shared optical networks*, IEEE LCN 2006 submission, <http://ecpe.ee.iastate.edu/dcn/DCNLWEB/Publications/docs/Conf-Pub/lcn2006.pdf>
- [14] K.Zhu et al, *A comprehensive study of next-generation optical grooming switches*, IEEE JSAC, Vol 21, No. 7, September 2002.
- [15] H.Zhu, H.Zang, K.Zhu, B.Mukherjee, *Dynamic traffic grooming in WDM mesh networks using a novel graph model*, IEEE Globecom 2004